AD-A193 000 COMPARISON OF EDGE DIFFRACTION THEORIES(U) NAVAL RESEARCH LAB WASHINGTON DC W B GORDON 10 MAR 88 NRL-MR-6169 1/1

UNCLASSIFIED F/G 20/6 NL

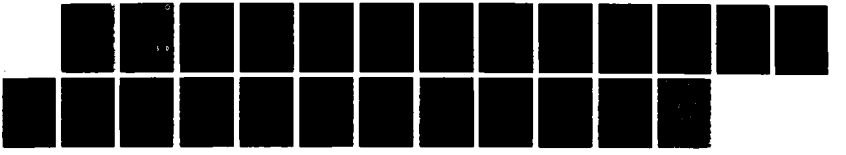

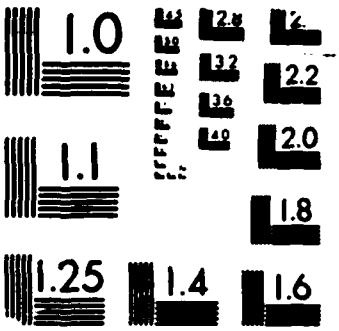

MICROCOPY RESOLUTION TEST CHART

Naval Research Laboratory
Washington, DC 20375-5000

(2)

NRL Memorandum Report 6169

Comparison of Edge Diffraction Theories

W. B. GORDON
Radar Analysis Branch
Radar Division

March 18, 1988

SECURITY CLASSIFICATION OF THIS PAGE

ADA193880

REPORT DOCUMENTATION PAGE

Form Approved
OMB No. 0704-0188

1a. REPORT SECURITY CLASSIFICATION UNCLASSIFIED	1b. RESTRICTIVE MARKINGS
2a. SECURITY CLASSIFICATION AUTHORITY	3. DISTRIBUTION/AVAILABILITY OF REPORT Approved for public release; distribution unlimited.
2b. DECLASSIFICATION/DOWNGRADING SCHEDULE	
4. PERFORMING ORGANIZATION REPORT NUMBER(S) NRL Memorandum Report 6169	5. MONITORING ORGANIZATION REPORT NUMBER(S)
6a. NAME OF PERFORMING ORGANIZATION Naval Research Laboratory 6b. OFFICE SYMBOL (If applicable)	7a. NAME OF MONITORING ORGANIZATION
6c. ADDRESS (City, State, and ZIP Code) Washington, D.C. 20375-5000	7b. ADDRESS (City, State, and ZIP Code)
8a. NAME OF FUNDING/SPONSORING ORGANIZATION Office of Naval Research 8b. OFFICE SYMBOL (If applicable)	9. PROCUREMENT INSTRUMENT IDENTIFICATION NUMBER
8c. ADDRESS (City, State, and ZIP Code) Arlington, VA 22217	10. SOURCE OF FUNDING NUMBERS PROGRAM ELEMENT NO. 61153N; PROJECT NO. RR0210 541; TASK NO.; WORK UNIT ACCESSION NO. EX280-340

11. TITLE (Include Security Classification)
Comparison of Edge Diffraction Theories

12. PERSONAL AUTHOR(S)
Gordon, W.B.

13a. TYPE OF REPORT	13b. TIME COVERED	14. DATE OF REPORT (Year, Month, Day)	15. PAGE COUNT
Interim	FROM 6/87 TO 1/87	1988 March 18	24

16. SUPPLEMENTARY NOTATION

17. COSATI CODES			18. SUBJECT TERMS (Continue on reverse if necessary and identify by block number)
FIELD	GROUP	SUB-GROUP	Physical Theory of Diffraction, Incremental Length Diffraction Coefficient, Method of Equivalent Currents

19. ABSTRACT (Continue on reverse if necessary and identify by block number)

We examine various edge diffraction theories for the calculation of electromagnetic scatter from flat plates. The theories are compared, their shortcomings are discussed, and possible remedies are briefly described.

20. DISTRIBUTION/AVAILABILITY OF ABSTRACT ☒ UNCLASSIFIED/UNLIMITED ☐ SAME AS RPT ☐ DTIC USERS	21. ABSTRACT SECURITY CLASSIFICATION UNCLASSIFIED
22a. NAME OF RESPONSIBLE INDIVIDUAL W.B. Gordon	22b. TELEPHONE (Include Area Code) (202) 767-2999 22c. OFFICE SYMBOL Code 5311

DD Form 1473, JUN 86

SECURITY CLASSIFICATION OF THIS PAGE

CONTENTS

1. INTRODUCTION 1

2. SUMMARY OF MAIN RESULTS 1

3. GRAPHICAL RESULTS AND ADDITIONAL COMMENTARY 2

4. REFERENCES 5

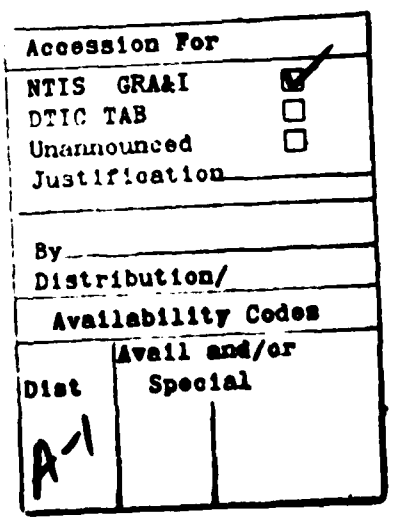

COMPARISON OF EDGE DIFFRACTION THEORIES

1. INTRODUCTION

In this report we shall examine Ufimtsev's Physical Theory of Diffraction (PTD) and Mitzner's Incremental Length Diffraction Coefficient Method (ILDC) for the calculation of edge scatter. These two theories are very similar (respectively) to Keller's Geometrical Theory of Diffraction and Michaeli's Method of Equivalent Currents, and as shown by Knott [1,2,3], these latter two theories differ from the former only in the way in which they do, or do not, incorporate physical optics (PO) effects explicitly in the solutions. In fact, the PTD and ILDC algorithms are applied to each edge of a plate (or wedge face), and the total scatter is then obtained by taking the coherent sum of all these edge contributions with the PO area scattering integral. To this recipe one must also add the effects of standing wave interaction effects, as will be discussed.

In our comparisons we shall use the PTD as modified by Knott in [1] and [2], and also the ILDC as described by Knott in [2] and [3]. The PO effects will be calculated according to vectorized versions of the formula's given by Gordon in [4], and also described by Knott in [1] and [2]. Finally, we mention that Michaeli has published a new version of his theory in a very recent paper [5], but that according to the evidence that Michaeli himself presents, the results do not appear to be in very good agreement with experimental values.

2. SUMMARY OF MAIN RESULTS

The results summarized below in this section will be illustrated by graphical results presented in the next section, along with additional commentary and references.

(1) Both the ILDC and PTD algorithms contain an irremovable singularity (pole) at grazing incidence in the forward scattering direction; i.e., the algorithms blow up when the incidence vector is parallel to the plate and the bi-static scattering angle is 180 degrees. This is a defect which all of these edge diffraction theories inherit from the original Sommerfeld "exact" solution to scattering by a semi-infinite plane or wedge [6]. The practical importance of this defect is that it prohibits the calculation of edge-to-edge interaction effects near grazing incidence, as will be discussed below.

(2) More generally, closed-form hand calculations reveal that the out-

Manuscript approved January 13, 1988.

puts from the ILDC and PTD are equal when the incidence and scatter vectors are perpendicular to the edge.

(3) Both the ILDC and PTD are numerically unstable near normal incidence to a wedge face. Hence it has been necessary to use double precision in both cases.

(4) There are some "apparent" singularities in the PTD and ILDC (where a singularity in one term is cancelled out by a singularity in another term). The resolution of these apparent sigularities requires a careful evaluation of limits, and complicates the computer coding by requiring the inclusion of special cases. Moreover, the coding for the ILDC formulas is further complicated by the existence of expressions for angles which are possibly imaginary in the general bistatic case. (Equations 5-52 and 5-53 in Ref. [2], or Equations 10 and 11 in Ref. [3]).

(5) Although there may be significant differences between the PTD and ILDC results for the scatter from a single edge, these differences tend to disappear when the total radar cross section (RCS) of a flat polygonal plate is estimated by adding the effects of all the edges to the PO surface effect.

(6) At certain polarizations one must also take into account the effects of standing wave interactions. However, to this author's best knowledge, a successful calculation of such interaction effects has been carried out in only one special case; viz., that of a rectangle when the line of incidence is perpendicular to two of the edges and parallel to the others. In this special case the PTD and ILDC theories give the same results.

To summarize, we conclude that although the PTD is somewhat easier to implement numerically than the ILDC, there does not appear to be, at present, any good reason to prefer one of these methods over the other: Both methods have singularities at grazing incidence; neither method has been successfully applied to the calculation of standing wave effects at arbitrary incidence; and both methods produce exactly the same results in the special case for which the calculation can be carried out (and experimental results exist. See the discussion below.)

3. GRAPHICAL RESULTS AND ADDITIONAL COMMENTARY

In the figures THETA is the off-normal angle to the face of a plate or wedge, PHI is an azimuthal angle which equals zero when the line of sight is perpendicular to an edge, and WANG is the interior wedge angle. Hence we set WANG = 0 when we calculate the scatter from a single flat plate. Edges are oriented so that an edge is a leading edge when THETA = -90 deg., and a trailing edge when THETA = +90 deg.

In all the figures shown below we only consider the case of monostatic backscatter.

The E(H) polarization case corresponds to the case when the E(H) vector is parallel to the plate or wedge face.

The first 8 figures show the scatter from a single edge as calculated by the ILDC (heavy line) and PTD (dotted line) algorithms. The calculations are carried out for two values of WANG (0 and 135 degrees) and four values of PHI (0, 30, 45, and 80 degrees). In Figures 1 and 5 PHI = 0, and the PTD and ILDC results are exactly the same. The maximum RCS predicted by both theories for monostatic scatter from an edge of length L is given by the frequency independent result

$$\sigma_{max} = L^2/\pi \quad .$$

For flat plates this maximum is only attained when the grazing angle is zero and the line-of-sight is perpendicular to an edge. Also, the E-vector must be parallel to a leading edge or perpendicular to a trailing edge. This maximum is shown in Figure 1 for the case of E-polarization. The corresponding curve for H-polarization can be obtained by reflecting the curve in Figure 1 about the axis THETA = 0.

Figure 9 shows what happens when the edge effects are added to the PO effect to obtain an estimate for the total RCS of a unit square. In these calculations the effects of edge-to-edge interactions are not taken into account. The dotted line shows the PO result and the heavy line shows the PO + ILDC result. The corresponding PO + PTD results is exactly the same and is therefore not shown. The corresponding calculated result for H-polarization is also the same; however it is known that there is a real physical difference between these two polarizations which can only be reproduced by taking into account the effects of edge-to-edge interactions. More specifically, the flat tails at grazing incidence shown in Figure 9 are known to be physically accurate for E-polarization, but the experimental curves for H-polarization tail-off to zero.

Experimental and theoretical curves for the scatter from flat plates have been published by Ross in [7]. We are referring specifically to Ross's figures 3,4,5 which depict the monostatic RCS of square plates as a function of THETA for the case when the line of incidence is perpendicular to an edge. These figures are not reproduced here because of their small size and fine detail; however, in the remaining figures of this report we have used the same height-to-width ratio as in the figures of Ross to facilitate a comparison between Ross's results and ours. We also note that the E- and H-polarization cases discussed here correspond to Ross's "vertical" and "horizontal" polarizations.

Ross obtained his theoretical curves by applying the Geometrical Theory of Diffraction (GTD) to the two dimensional problem of diffraction by a semi-infinite strip, and then applying a "scaling law" to reduce the RCS so obtained (having the dimensions of length) to an RCS having the dimensions of length-squared. This method is only applicable when the line-of-sight is perpendicular to one pair of edges. In this case the standing wave effects are represented as interactions between the edges, and the more general case would seem to require that the GTD, PTD, or ILDC be recast into a form involving vertex diffraction, as is suggested by the generalized Fermat Principle which motivates the GTD [8, 9].

We are frankly at a loss to understand how Ross calculated the edge-to-

edge interactions for E-polarization, since in this case the classical diffraction coefficients of Sommerfeld vanish for a surface wave propagating from one edge to the opposite edge. In other words, according to our understanding, there should be no edge-to-edge effects for this polarization. At any rate, according to Ross's figures the edge-to-edge effects are very small for E-polarization, except near grazing incidence where they produce a singularity.

Figures 10-12 show the results of our calculation of edge-to-edge effects by the straightforward use of the PTD algorithm in the H-polarization case. The parameters (radar wavelength and side of square in meters) are the same as in the corresponding figures of Ross.

The curves labeled "no interactions" show the results of adding the PO scatter to the direct edge scatter (with no edge-to-edge interactions). Hence, these curves can also be taken to represent the total RCS in the E-polarization case because (according to our understanding) there are no edge-to-edge interaction effects for E-polarized waves and because the direct edge effects for both polarizations are exactly the same. These curves are in good agreement with Ross's "experimental" curves for E-polarization, and moreover do not contain the singularities at grazing incidence that occur in Ross's calculations.

The curves labeled "1st order interactions" contain the effects of rays which proceed from the radar, hit an edge, propagate across the surface to the opposite edge, and then return to the radar. Higher order interactions correspond to rays which propagate back-and-forth between two opposite edges before returning to the radar, but from the figures it can be seen that the second order interactions have almost no effect. The curves involving interactions contain a singularity at grazing incidence because of the fundamental defect which these edge theories inherit from the Sommerfeld solution.

In the PTD calculation a wave propagated from an edge to the opposite edge is attenuated (in amplitude) by a factor proportional to (L/R), where L is the edge width and R is the distance to the opposite edge. This a far-field result whose accuracy requires that this factor be small, which is not the case for squares. In fact, we have found that the accuracy of the PTD results in this case can be improved by certain modifications for which we have not theoretical justification. First, we arbitrarily increase the propagation factor by a factor of 2. This modification improves the behavior at the inner sidelobes. Second, we multiply the radiation amplitude pattern by a tapering factor equal to $\cos^2 \theta$ across the entire range of θ. More specifically, referring to the diffraction coefficients f and g discussed by Knott in [1,2,3], we multiply the g coefficient by this taper. This second modification has a small effect on the inner sidelobes and causes the calculated radiation pattern to vanish at the tails in the H-polarization case. (It also has a very slight effect on the E-polarization calculations.) However, the end lobes (near grazing incidence) produced by this method are lower and narrower that the end lobes seen in Ross's experimental curves. The results of these modifications are shown in Figures 13-15.

4. REFERENCES

(1) E. F. Knott, A progression of high-frequency RCS prediction techniques, Proc. IEEE 73 (1985), p. 252-264.

(2) E. F. Knott, et al., Radar Cross Section, Artech 1985.

(3) E. F. Knott, The relationship between Mitzner's ILDC and Michaeli's Equivalent Currents, IEEE Trans. AP-33 (Jan. 1985), p. 112-114.

(4) W. B. Gordon, Far-field approximations to the Kirchhoff-Helmholtz representations of scattered field, IEEE Trans. AP-23 (1975), 590-592.

(5) A. Michaeli, Equivalent currents for second order diffraction by the edges of perfectly conducting polygonal surfaces, IEEE Trans. AP-85 (1987), p. 183-190.

(6) M. Born and E. Wolf, PRinciples of Optics, 5'th ed., Pergamon Press, Oxford, 1975.

(7) R. A. Ross, Radar cross section of rectangular flat plates as a function of aspect angle, IEEE Trans. AP-14, (1966), p. 329-335.

(8) J. B. Keller, Geometrical theory of diffraction, J. Opt. Soc. of Am. 52 (1962), p. 116-130.

(9) J. B. Keller, Rays, waves and asymptotics, Bull. Am. Math. Soc. 84 (1978), p. 727-750.

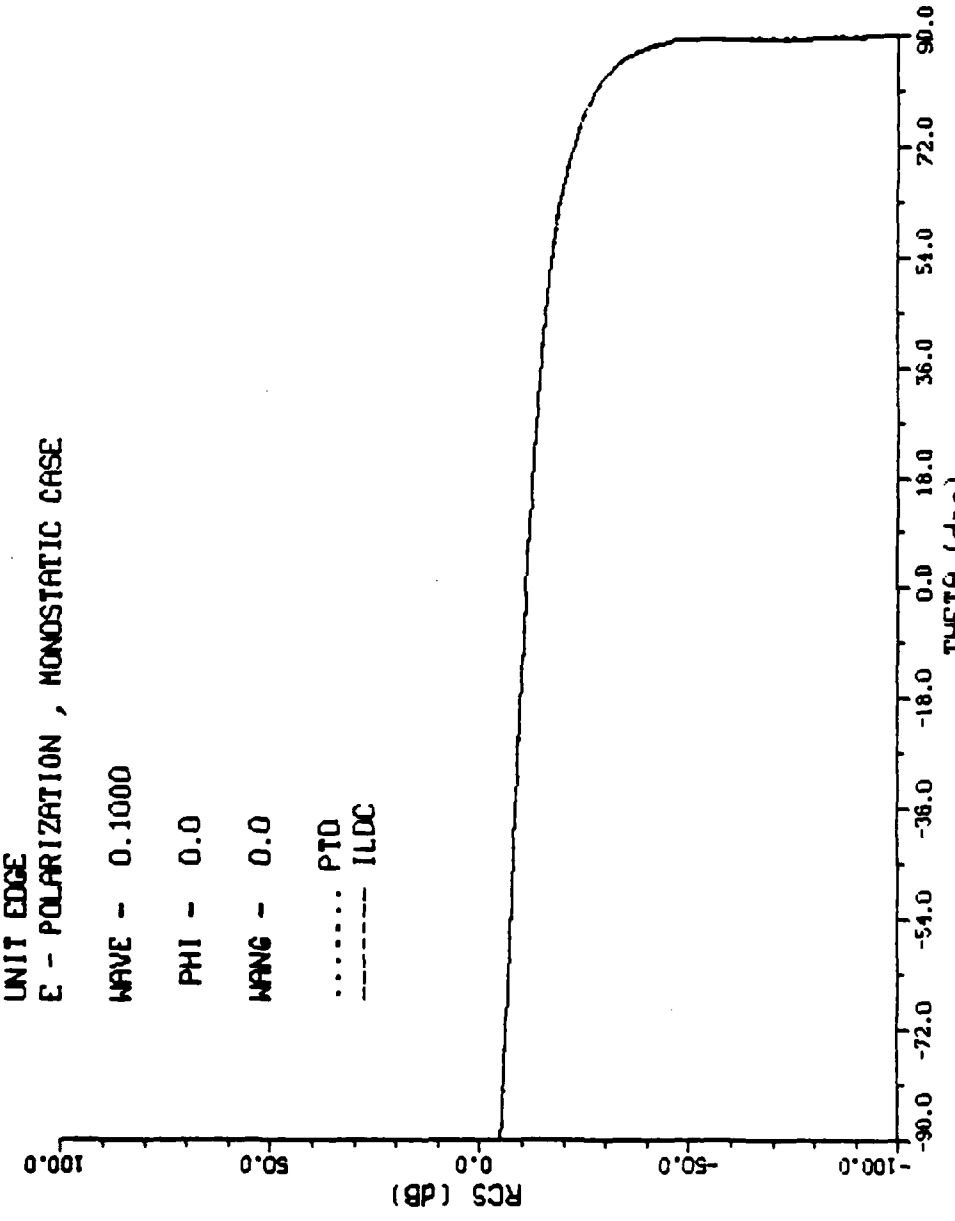
UNIT EDGE
E - POLARIZATION , MONOSTATIC CASE
WAVE - 0.1000
PHI - 0.0
WANG - 0.0
..... PTD
------ ILDC
RCS (dB)
100.0
50.0
0.0
-50.0
-100.0
-90.0
-72.0
-54.0
-36.0
-18.0
0.0
18.0
36.0
54.0
72.0
90.0
THETA (deg)

Figure 1

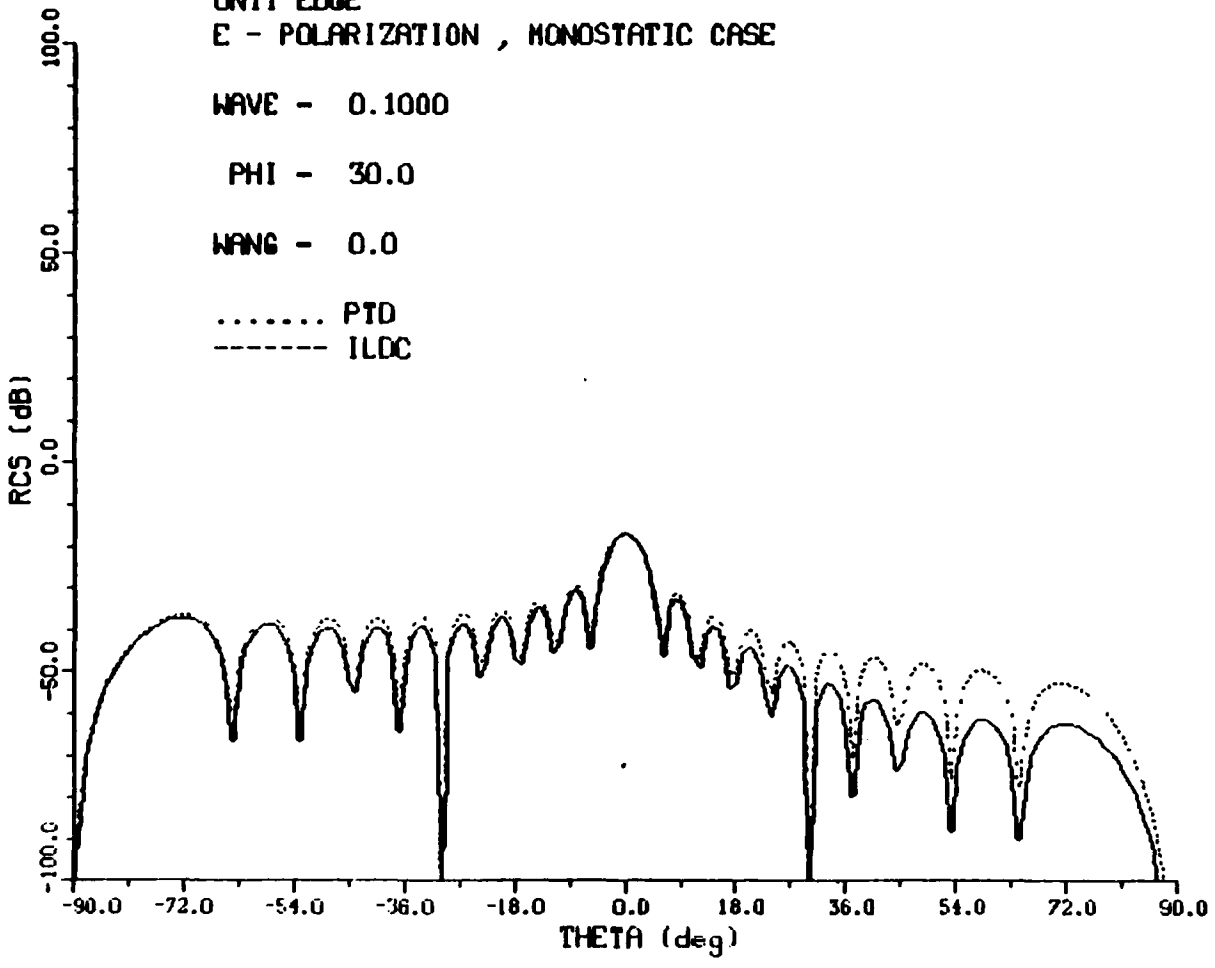
UNIT EDGE
E - POLARIZATION , MONOSTATIC CASE
WAVE - 0.1000
PHI - 30.0
WANG - 0.0
..... PTD
------- ILDC
RCS (dB)
100.0
50.0
0.0
-50.0
-100.0
-90.0
-72.0
-54.0
-36.0
-18.0
0.0
18.0
36.0
54.0
72.0
90.0
THETA (deg)

Figure 2

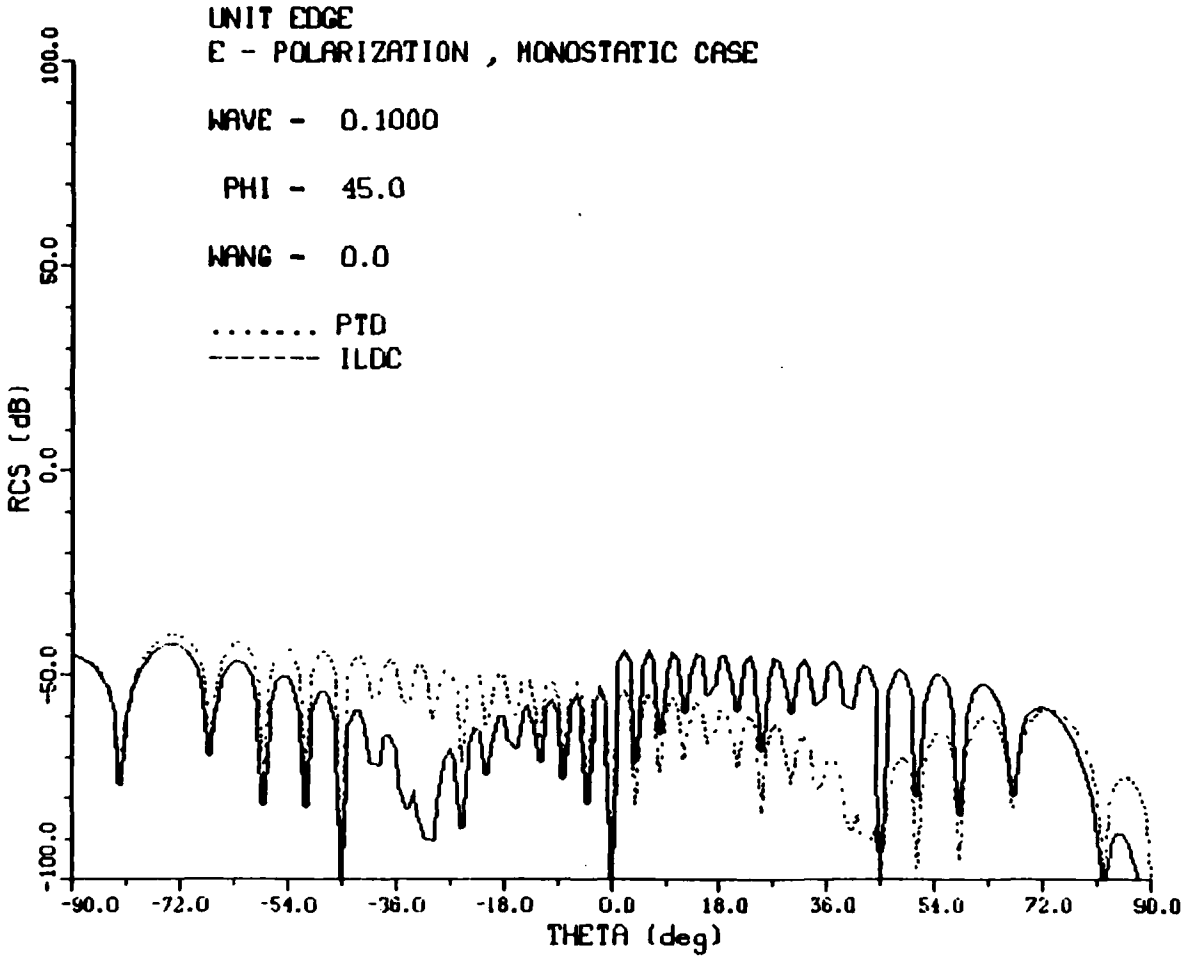
UNIT EDGE
E - POLARIZATION , MONOSTATIC CASE
WAVE - 0.1000
PHI - 45.0
WANG - 0.0
..... PTD
------- ILDC
RCS (dB)
100.0
50.0
0.0
-50.0
-100.0
-90.0
-72.0
-54.0
-36.0
-18.0
0.0
18.0
36.0
54.0
72.0
90.0
THETA (deg)

Figure 3

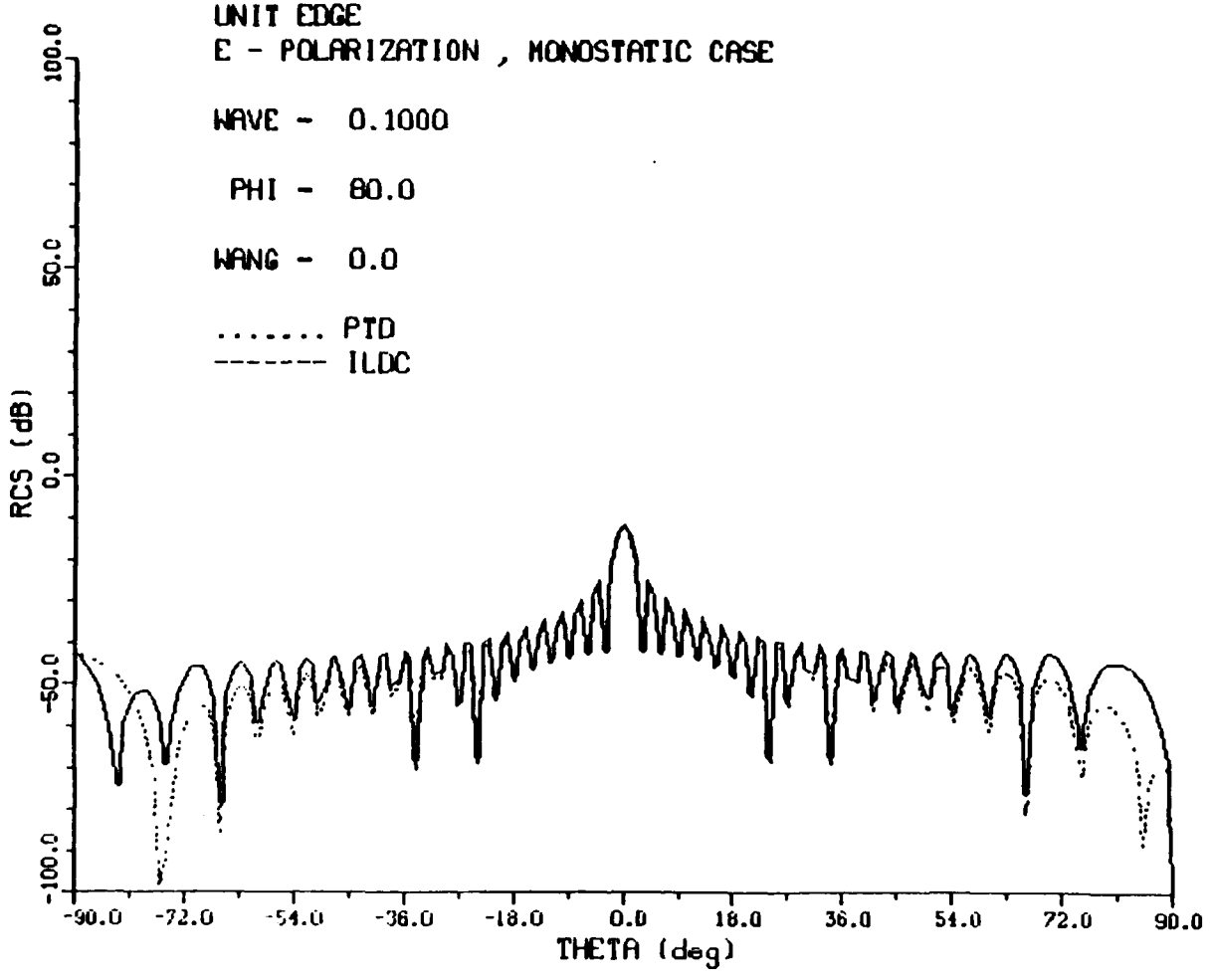
UNIT EDGE
E - POLARIZATION , MONOSTATIC CASE
WAVE - 0.1000
PHI - 80.0
WANG - 0.0
..... PTD
------- ILDC
RCS (dB)
100.0
50.0
0.0
-50.0
-100.0
-90.0
-72.0
-54.0
-36.0
-18.0
0.0
18.0
36.0
54.0
72.0
90.0
THETA (deg)

Figure 4

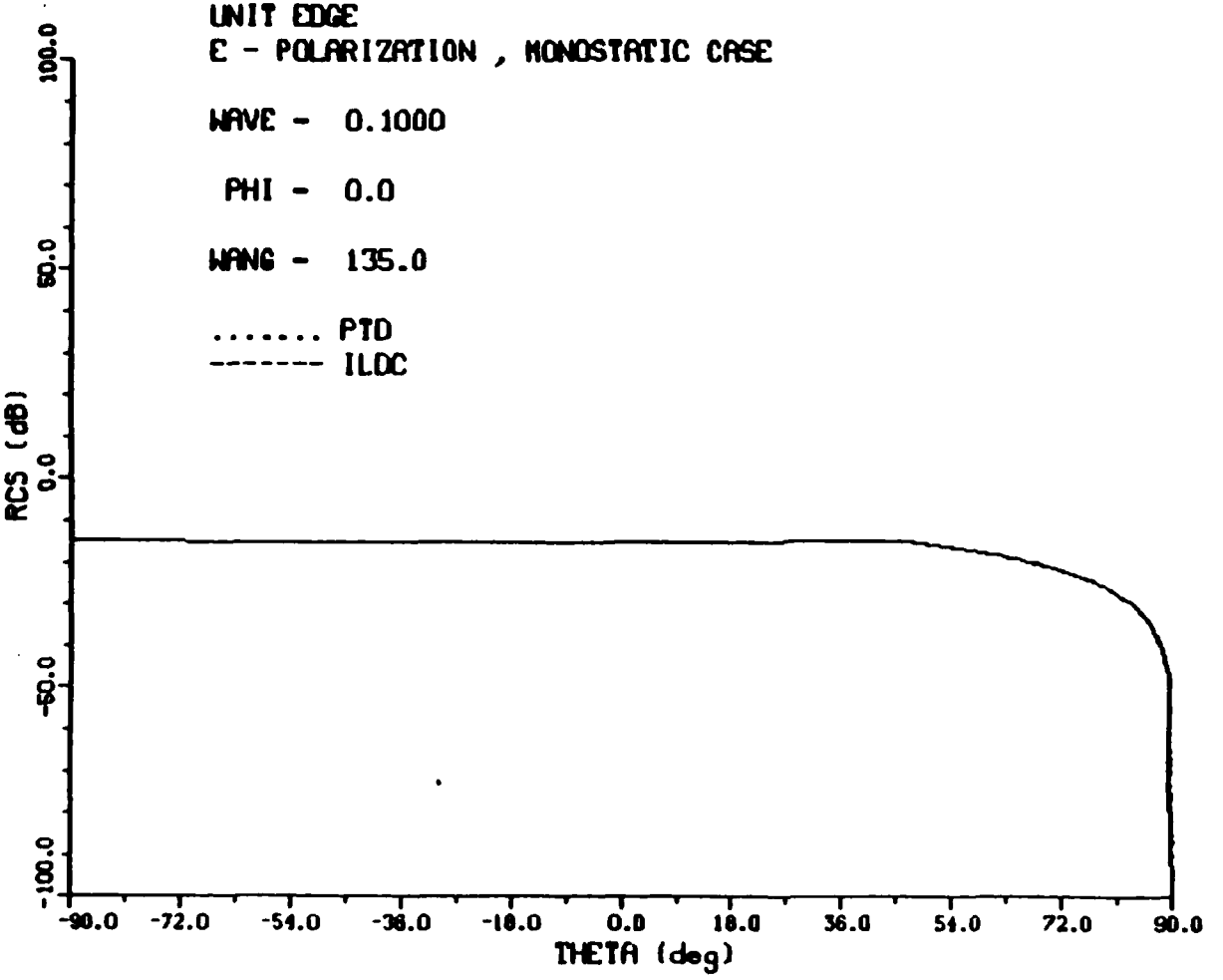
UNIT EDGE
E - POLARIZATION , MONOSTATIC CASE
WAVE - 0.1000
PHI - 0.0
WANG - 135.0
..... PTD
------- ILDC
RCS (dB)
100.0
50.0
0.0
-50.0
-100.0
-90.0
-72.0
-54.0
-36.0
-18.0
0.0
18.0
36.0
54.0
72.0
90.0
THETA (deg)

Figure 5

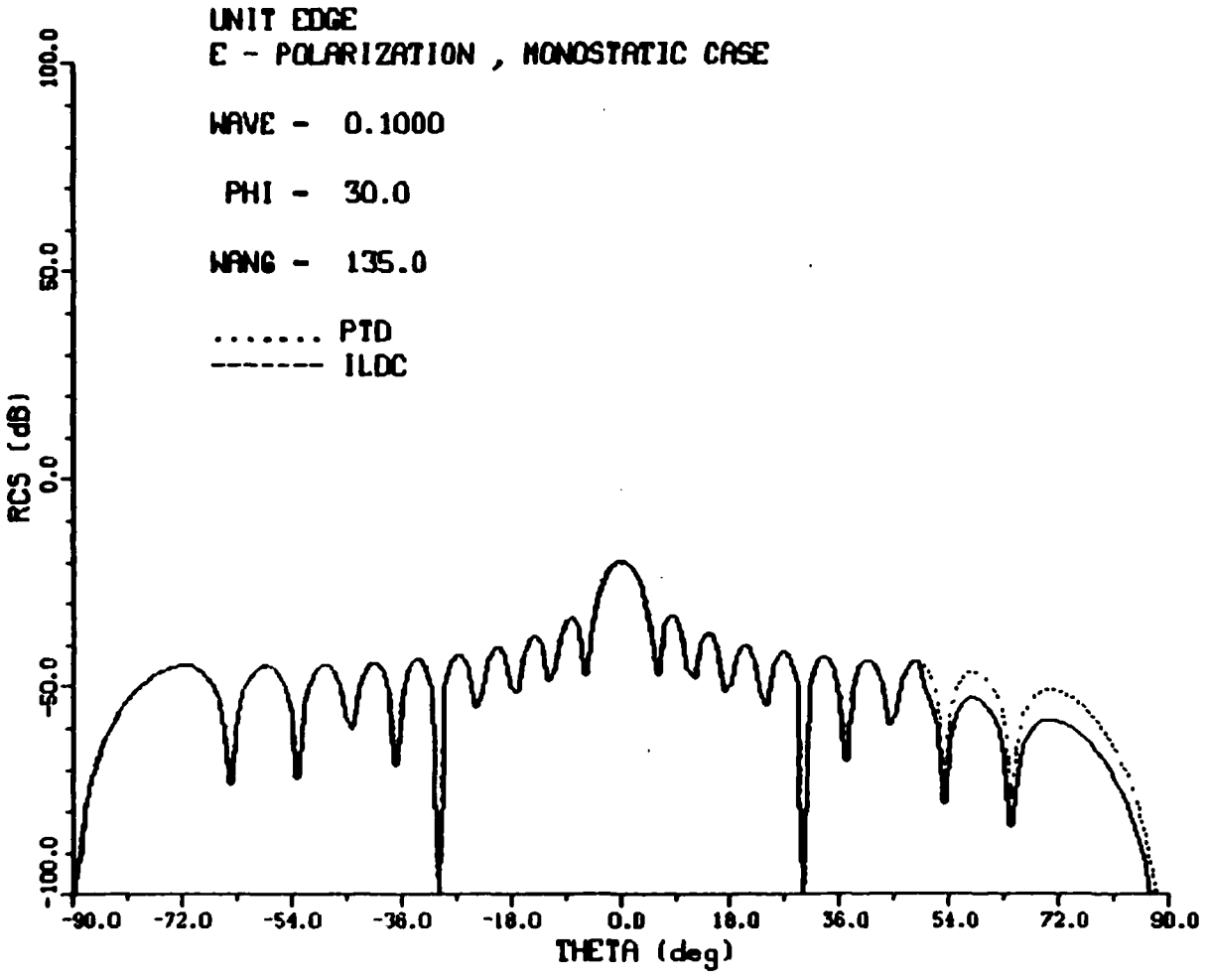
UNIT EDGE
E - POLARIZATION , MONOSTATIC CASE
WAVE - 0.1000
PHI - 30.0
WANG - 135.0
..... PTD
------- ILDC
RCS (dB)
100.0
50.0
0.0
-50.0
-100.0
-90.0
-72.0
-54.0
-36.0
-18.0
0.0
18.0
36.0
54.0
72.0
90.0
THETA (deg)

Figure 6

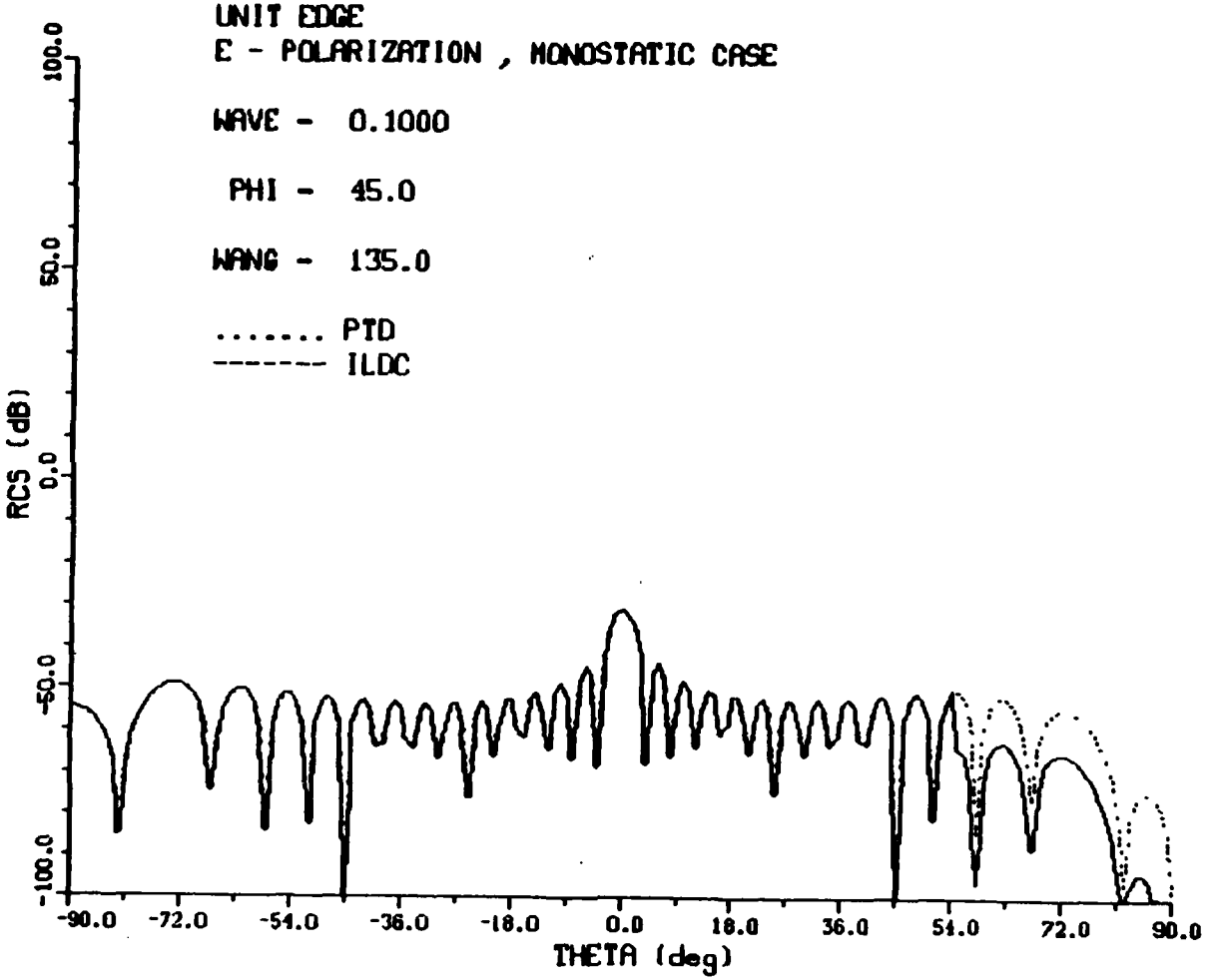
UNIT EDGE
E - POLARIZATION , MONOSTATIC CASE
WAVE - 0.1000
PHI - 45.0
WANG - 135.0
..... PTD
------- ILDC
RCS (dB)
100.0
50.0
0.0
-50.0
-100.0
-90.0
-72.0
-54.0
-36.0
-18.0
0.0
18.0
36.0
54.0
72.0
90.0
THETA (deg)

Figure 7

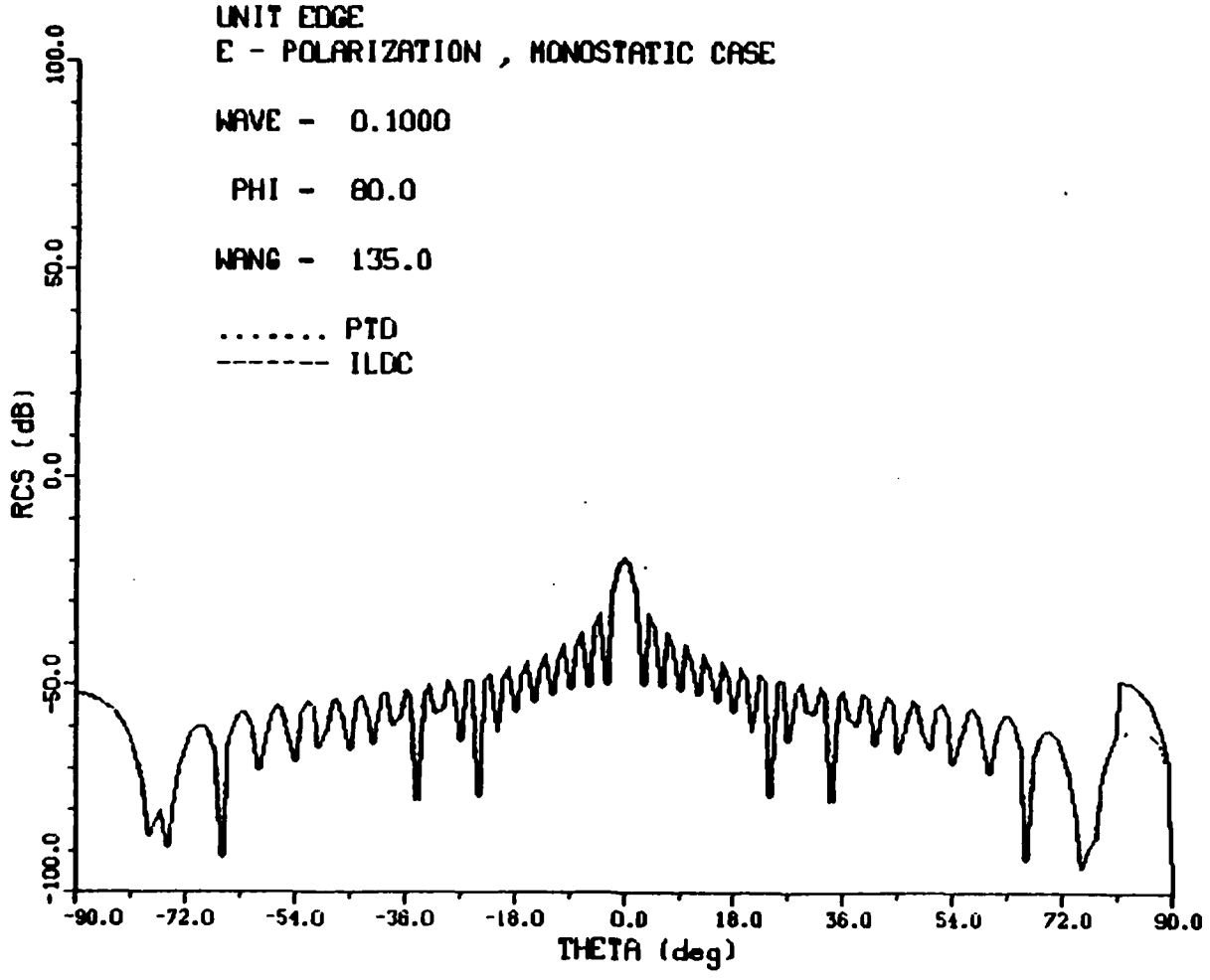
UNIT EDGE
E - POLARIZATION , MONOSTATIC CASE
WAVE - 0.1000
PHI - 80.0
WANG - 135.0
..... PTD
------- ILDC
RCS (dB)
100.0
50.0
0.0
-50.0
-100.0
-90.0
-72.0
-54.0
-36.0
-18.0
0.0
18.0
36.0
54.0
72.0
90.0
THETA (deg)

Figure 8

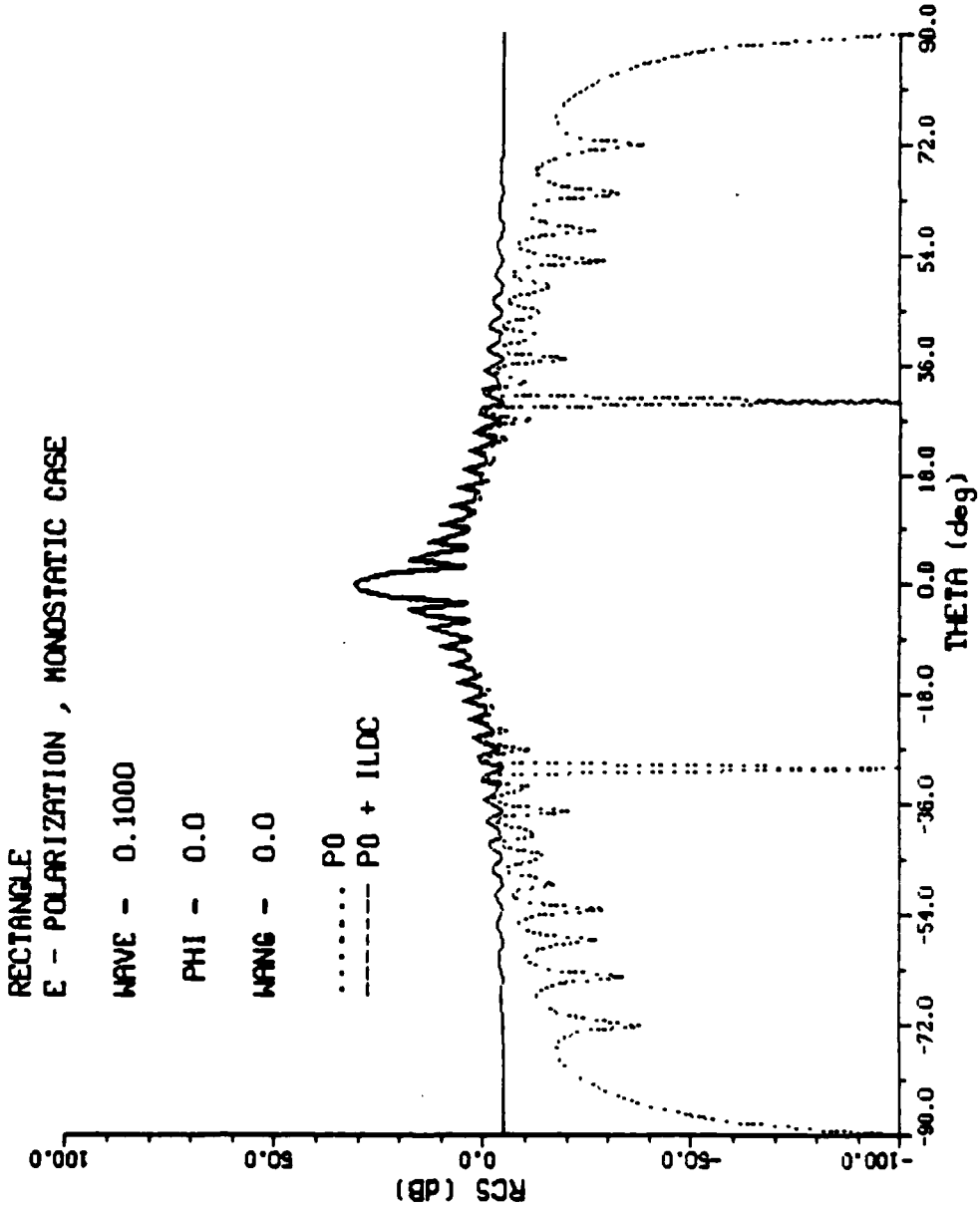
RECTANGLE
E - POLARIZATION , MONOSTATIC CASE
WAVE - 0.1000
PHI - 0.0
WANG - 0.0
PO
PO + ILDC
RCS (dB)
100.0
50.0
0.0
-50.0
-100.0
-90.0
-72.0
-54.0
-36.0
-18.0
0.0
18.0
36.0
54.0
72.0
90.0
THETA (deg)

Figure 9

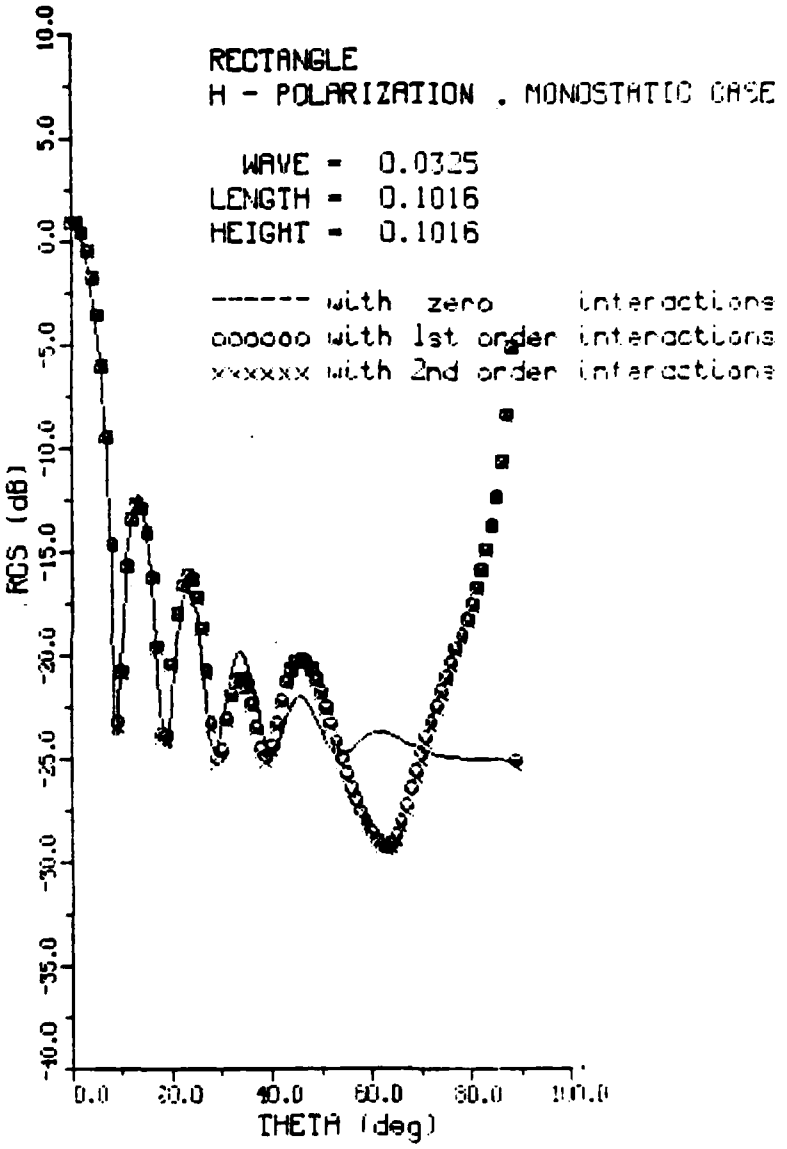
RECTANGLE
H - POLARIZATION . MONOSTATIC CASE
WAVE = 0.0325
LENGTH = 0.1016
HEIGHT = 0.1016
------ with zero interactions
oooooo with 1st order interactions
xxxxxx with 2nd order interactions
RCS (dB)
10.0
5.0
0.0
-5.0
-10.0
-15.0
-20.0
-25.0
-30.0
-35.0
-40.0
0.0
20.0
40.0
60.0
80.0
100.0
THETA (deg)

Figure 10

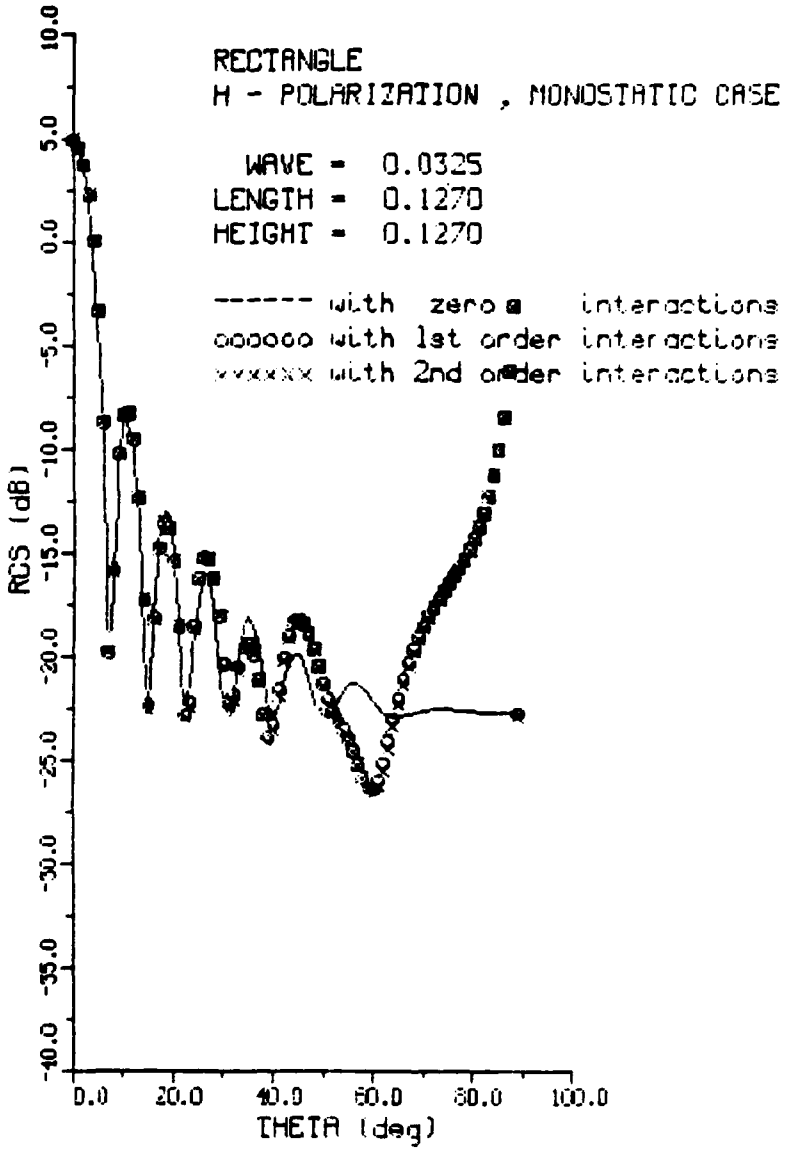
RECTANGLE
H - POLARIZATION , MONOSTATIC CASE
WAVE = 0.0325
LENGTH = 0.1270
HEIGHT = 0.1270
------ with zero interactions
oooooo with 1st order interactions
xxxxxx with 2nd order interactions
RCS (dB)
10.0
5.0
0.0
-5.0
-10.0
-15.0
-20.0
-25.0
-30.0
-35.0
-40.0
0.0
20.0
40.0
60.0
80.0
100.0
THETA (deg)

Figure 11

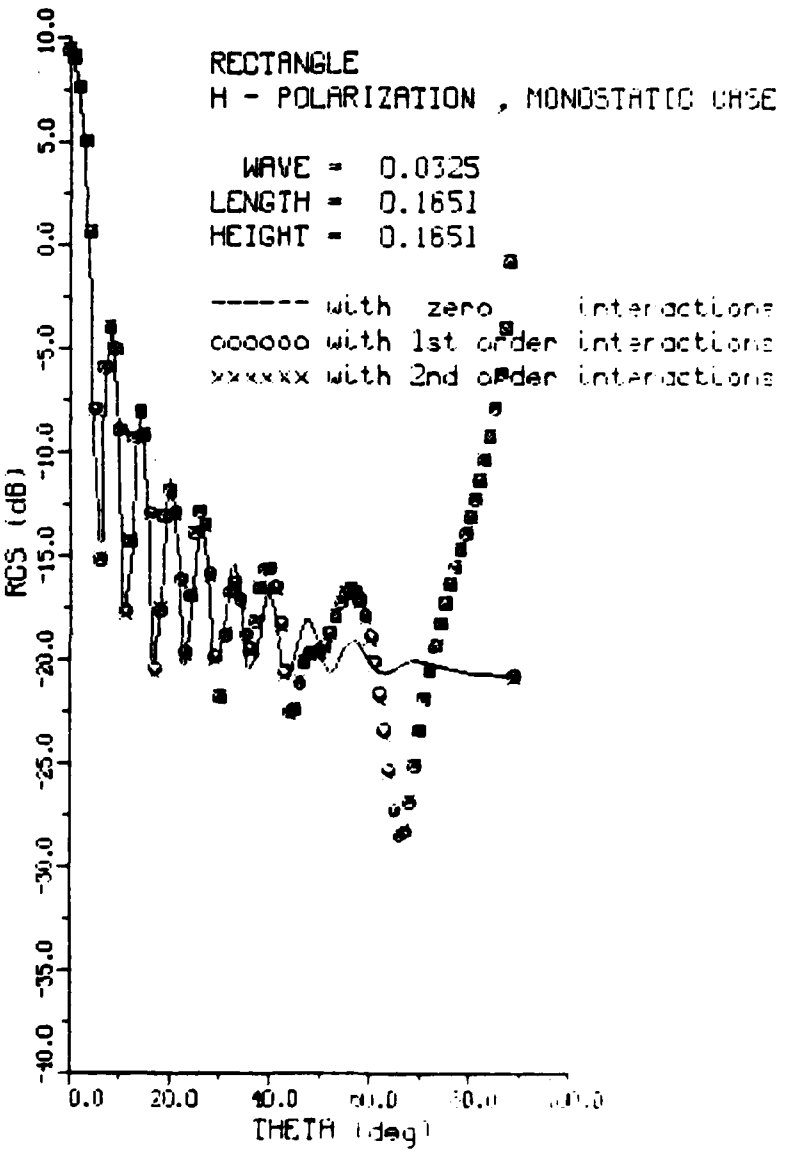
RECTANGLE
H - POLARIZATION , MONOSTATIC CASE
WAVE = 0.0325
LENGTH = 0.1651
HEIGHT = 0.1651
------ with zero interactions
oooooo with 1st order interactions
xxxxxx with 2nd order interactions
RCS (dB)
10.0
5.0
0.0
-5.0
-10.0
-15.0
-20.0
-25.0
-30.0
-35.0
-40.0
0.0
20.0
40.0
THETA (deg)

Figure 12

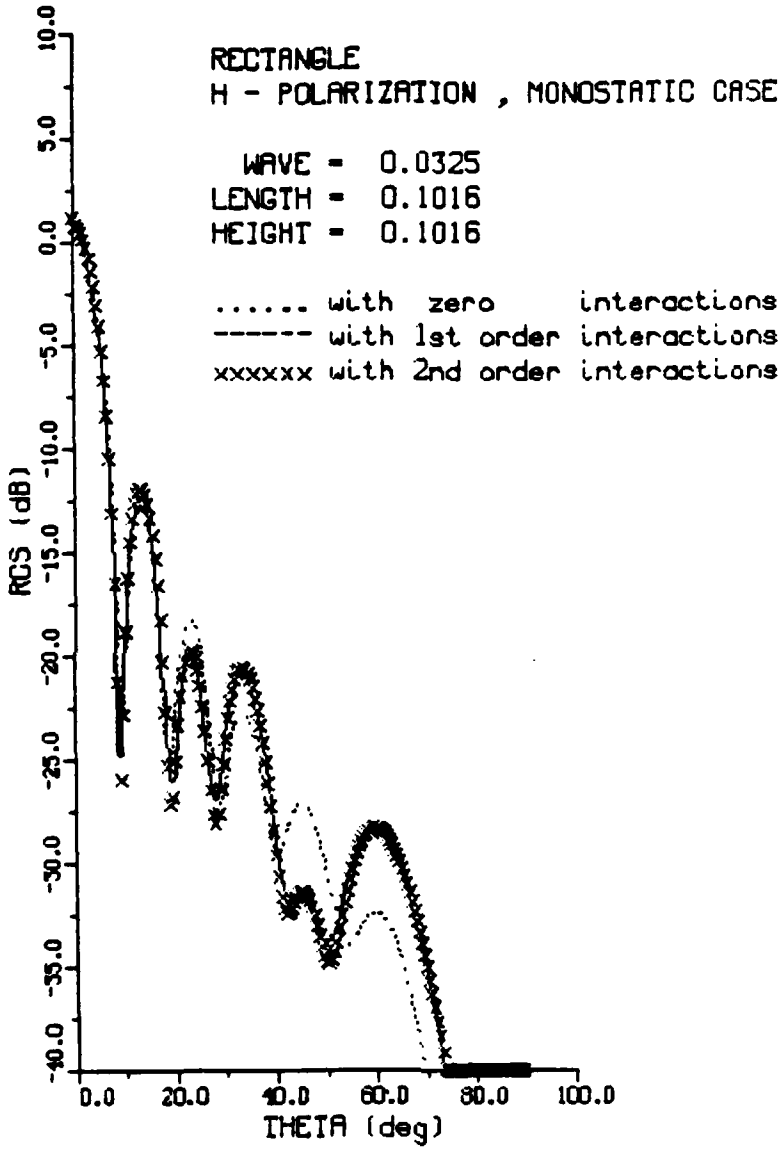
RECTANGLE
H - POLARIZATION , MONOSTATIC CASE
WAVE = 0.0325
LENGTH = 0.1016
HEIGHT = 0.1016
..... with zero interactions
------ with 1st order interactions
xxxxxx with 2nd order interactions
RCS (dB)
10.0
5.0
0.0
-5.0
-10.0
-15.0
-20.0
-25.0
-30.0
-35.0
-40.0
0.0
20.0
40.0
60.0
80.0
100.0
THETA (deg)

Figure 13

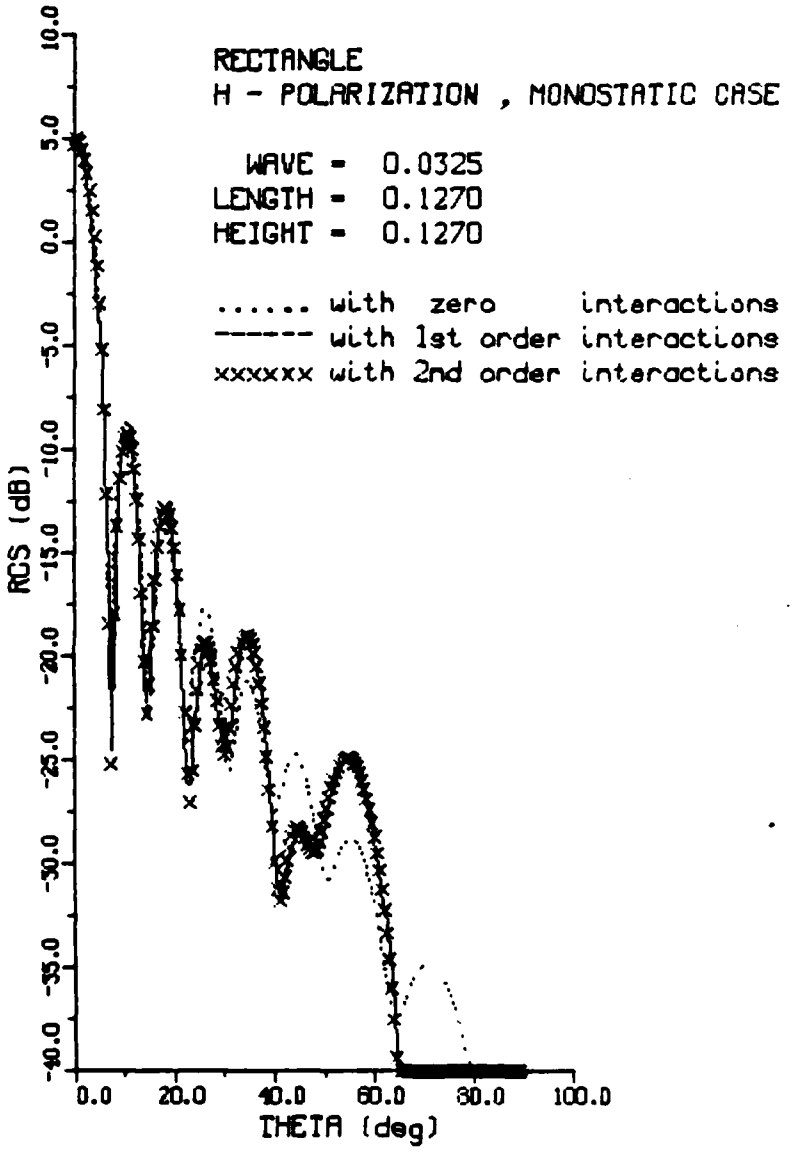
RECTANGLE
H - POLARIZATION , MONOSTATIC CASE
WAVE = 0.0325
LENGTH = 0.1270
HEIGHT = 0.1270
..... with zero interactions
------ with 1st order interactions
xxxxxx with 2nd order interactions
RCS (dB)
10.0
5.0
0.0
-5.0
-10.0
-15.0
-20.0
-25.0
-30.0
-35.0
-40.0
0.0
20.0
40.0
60.0
80.0
100.0
THETA (deg)

Figure 14

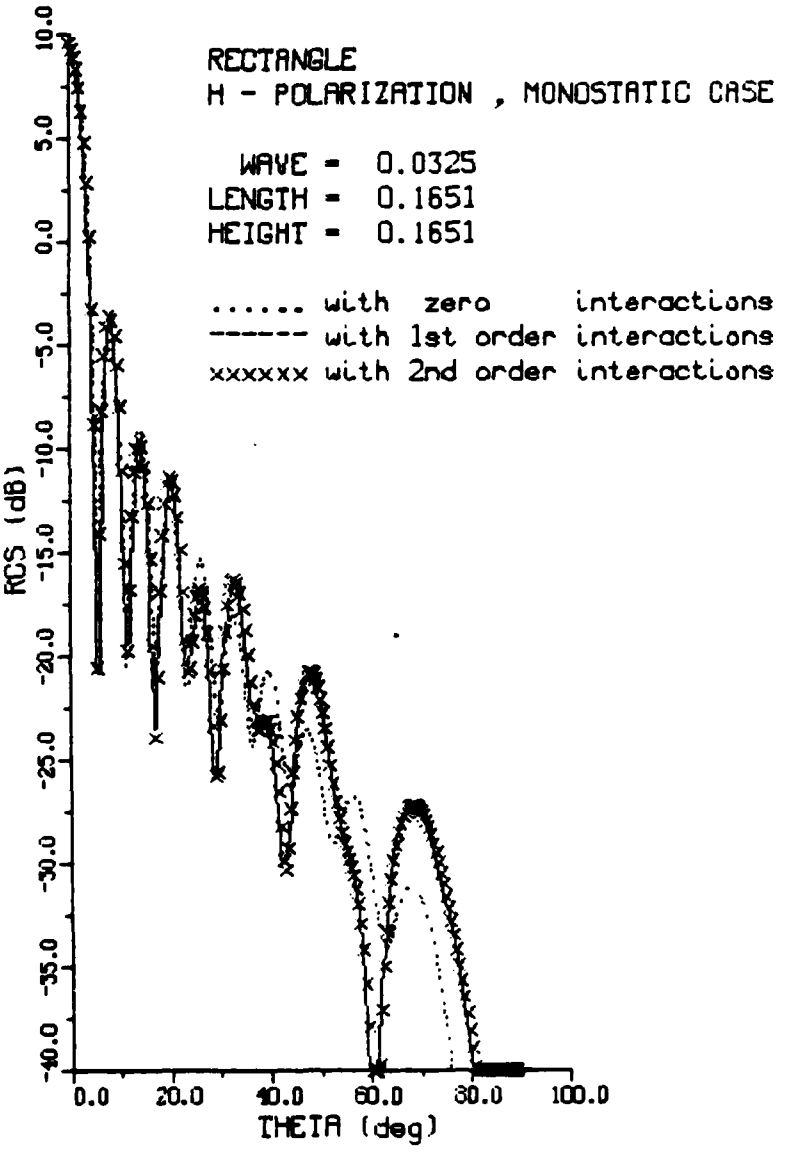
RECTANGLE
H - POLARIZATION , MONOSTATIC CASE
WAVE = 0.0325
LENGTH = 0.1651
HEIGHT = 0.1651
..... with zero interactions
------ with 1st order interactions
xxxxxx with 2nd order interactions
RCS (dB)
10.0
5.0
0.0
-5.0
-10.0
-15.0
-20.0
-25.0
-30.0
-35.0
-40.0
0.0
20.0
40.0
60.0
80.0
100.0
THETA (deg)

Figure 15

END

DATE

FILMED

8-88

DTIC